

Supporting Information.

1.- P(NIPAM-AAS) microgels synthesis.

P(NIPAM) microgels were prepared by surfactant free radical polymerization of 50 mL of an aqueous solution formed by *N*-isopropyl-acrylamide (0.1 M, 550 mg) and *N,N*-methylene-bis-acrylamide (0.007 M, 50 mg) at 70 °C using 250 mg of ammonium persulfate as initiator. With the aim of creating carboxylic group-rich shell in which the iron nanoparticles could be deposited, we added sodium acrylate (0.01 M, 35 mg) 15 min after starting the reaction (when the solution turns from transparent to white). This resulted in microgels enriched with carboxylic groups, which were preferentially distributed on the surface. Thus, the superficial negative charge of the microgels increased from 4.7 C/g for poly(NIPAM) microgels to 27.6 C/g for poly(NIPAM-AAS) microgels. After the addition of the acrylate monomer the mixture was refluxed for 4 h in N₂ atmosphere.

The product of this reaction was filtered and dialyzed against distilled water using a dialysis membrane (MWCO 12000-14000) for at least 2 days. During this period the water is frequently changed (at least 4 times). With this procedure unreacted monomers and oligomers are removed as indicated by the disappearance of the intense smell of NIPAM monomer coming from the microgels dispersion. To collect the dialyzed microgels, we centrifuge the dispersion at 5.000 rpm for 2 hours at room temperature. The monodisperse microgels obtained were finally freeze-dried and stored at room temperature.

In order to cover the P(NIPAM-AAS) microgels with iron oxide nanoparticles 0.1 g of P(NIPAM-AAS) microgels were dispersed in 50 mL of NaOH (0.1 M) aqueous solution. Afterwards, 50 mL of a HCl solution (0.1 M) in which we had previously dissolved 32.5 mg (0.18 mmol) of FeCl₃·6H₂O and 12 mg (0.09 mmol) of FeCl₂·4H₂O (Fe^{II}/Fe^{III} molar ratio = 0.5) was slowly added drop wise to the microgel dispersion under continuous stirring at 25 °C. At the end of this process the milky microgel dispersion turned to red-orange, indicating iron oxide formation. Changing the ratio microgels/iron is possible to modify the inorganic content of the hybrid material. Table 1 shows the concentration of each component used in the production of microgels with different concentration of iron oxide.

Table 1. Concentration of each component used in the production of the magnetic microgels.

P(NIPAM-AAS) microgels (mg)	FeCl ₂ ·4H ₂ O (mmol)	FeCl ₃ ·6H ₂ O (mmol)	γ-Fe ₂ O ₃ (%) obtained from TGA	Sample name
100	0.09	0.18	10	Fe10-P(NIPAM-AAS)
100	0.18	0.36	18	Fe18-P(NIPAM-AAS)
100	0.24	0.54	28	Fe28-P(NIPAM-AAS)
100	0.36	0.72	38	Fe38-P(NIPAM-AAS)

2.- Microgels characterization.

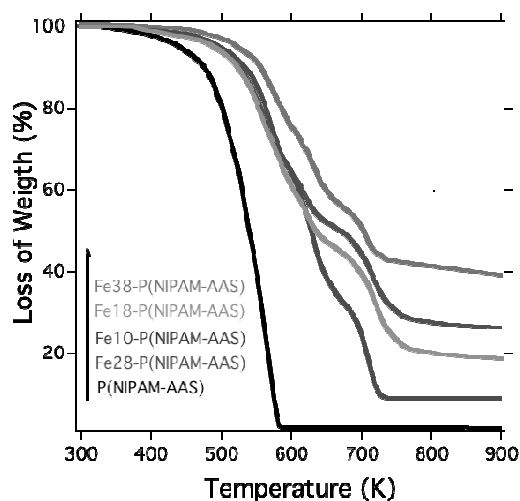


Fig. 1 Weight loss of P(NIPAM-AAS) microgels with varying amount of γ -Fe₂O₃ nanoparticles inside. The experiments were performed under air atmosphere at a heating rate of 10 °C per minute.

The Fig. 1 shows the weight loss of the different PNIPAM microgels as a function of temperature. The temperature for the maximum weight-loss rate increases with the amount of γ -Fe₂O₃ incorporated within the microgel. From the TGA measurements we obtained the amount of iron oxide incorporated in the microgels.

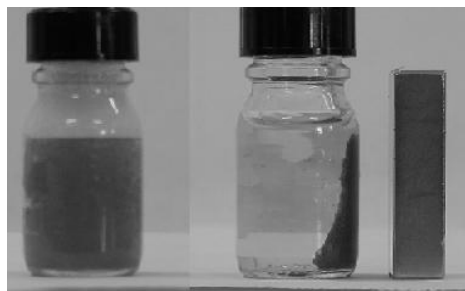


Fig. 2 Aqueous dispersion of magnetic microgels in the absence (left), and in the presence (right) of a magnet of 0.24T.

The magnetic response of the Fe28-P(NIPAM-AAS) microgels is illustrated in Fig.2. The hybrid microgels are dispersed in water (Fig.2 left side) but form a film on the flash wall following the magnetic field lines when a magnet of 0.24 T is approached (Fig.2 right side). Fig. 3 shows the dependence at 298 K of the hydrodynamic diameter with the iron content.

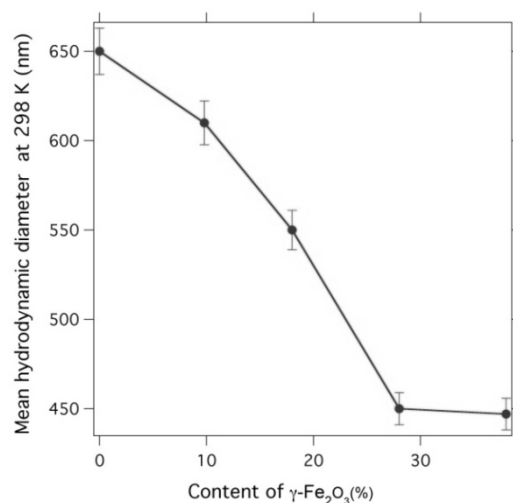


Fig.3 Hydrodynamic diameter at 298 K of the core-shell P(NIPAM-Acrylate) microgels as a function of the $\gamma\text{-Fe}_2\text{O}_3$ content. The error bars represent the standard deviation of three independent measurements for each point.

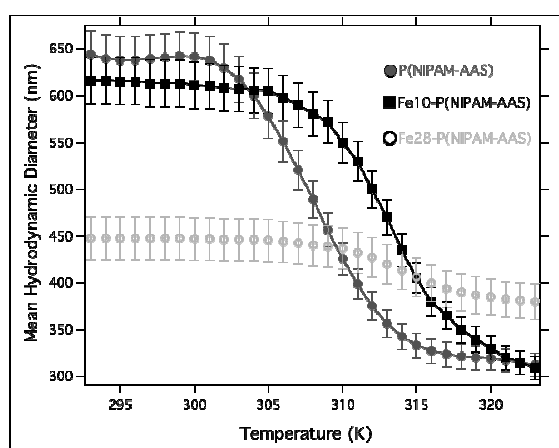


Fig. 4 Experimental mean particle diameter vs. temperature for different microgels as a function of the temperature; full dots P(NIPAM-AAS); full squares, Fe10-P(NIPAM-AAS) microgels; empty dots, Fe28-P(NIPAM-AAS) microgels. The error bars represent the standard deviation of three independent measurements for each point.

Fig.4 depicts the mean hydrodynamic diameter of different microgels as a function of temperature. At 298 K, in the swollen state of the microgels, the mean particle diameter is 640 ± 80 nm for P(NIPAM-AAS); 610 ± 85 nm for Fe10-P(NIPAM-AAS); and 450 ± 90 nm for Fe28-P(NIPAM-AAS).

3.- Derivation of the mean square displacement from neutron elastic scattering measurements.

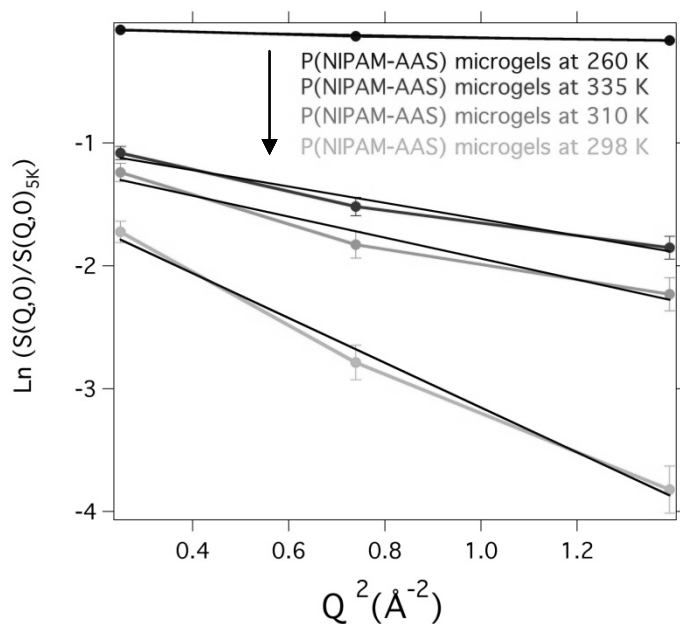


Fig. 5 Logarithm of the normalized elastic scattering intensity from IN10 backscattering spectrometer vs Q^2 for P(NIPAM-AAS) microgels at different temperatures.

4.- Molar fractions of different species obtained from FTIR data

The molar fraction of each species estimated by using the value of the relative absorptivity is plotted against the γ - Fe_2O_3 content in Fig. 6.

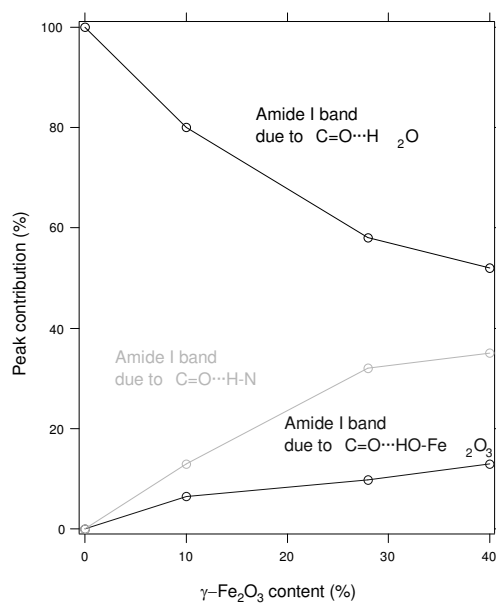


Fig. 6 Molar fraction of the C=O group of hybrid microgels that forms hydrogen bonds with water molecules, HN- groups of the polymer, and HO groups of γ -Fe₂O₃ nanoparticles as a function of the γ -Fe₂O₃ content.